# Density Functional Study of Ethylene Dimerization by (Acetylacetonato)nickel Hydride

**L. Fan,† A. Krzywicki,† A. Somogyvari,† and T. Ziegler*,‡**

Novacor Research & Technology Corporation, Calgary, Alberta, Canada T2E 7K7, and Department of Chemistry, University of Calgary, Calgary, Alberta, Canada T2N 1N4

*Received December 6, 1993*[⊗]

Density functional calculations have been carried out on the thermochemical aspects of catalytic ethylene dimerization by the $d^8$ hydride (propanedialato(1−))Ni−H (**I**), where the propanedialate(1−) anion served as a model for the chelate acac ligand, acetylacetonate(1−). The hydride (**I**) was found to have a low-spin $d^8$ configuration with a square planar structure where one site is vacated cis to hydrogen. It was shown that ethylene inserts readily into the Ni−H bond of (**I**) with an exothermicity of 44.6 kcal/mol. The resulting ethyl complex (**III**) has a strong agostic interaction between nickel and a $\beta$-hydrogen. It is suggested that the ethyl complex is the actual catalyst in the dimerization cycle. The agostic interaction in **III** is estimated to have a strength of 10 kcal/mol. The next insertion of ethylene into the Ni−ethyl bond of **III** leads to the butyl complex (**IV**). The insertion is exothermic by 25 kcal/mol. The reaction between (**IV**) and ethylene leads finally to the release of 1-butene and the regeneration of the ethyl complex (**III**). This step is nearly thermoneutral with a reaction heat of 0.1 kcal/mol. It is suggested that the elimination of 1-butene takes place via a transition state in which both ethylene and 1-butene are $\pi$-complexed to **I**. The internal barrier of activation for the final step is calculated to be 17 kcal/mol. The substitution of hydrogen by $CH_3$ or $CF_3$ groups on the propanedialate(1−) ligand were also considered. It was found that such substitutions only had a minor effect on the thermochemistry of the insertion processes in the dimerization cycle.

## 1. Introduction

Dimerization of ethylene to 1-butene or oligomerization of ethylene to higher linear α-olefins are both processes of considerable industrial importance. The linear oligomers are widely used in the synthesis of detergents or plasticizers, while 1-butene is an important comonomer in the production of linear low density polyethylenes. It is possible to synthesis α-olefins by catalytic cracking or pyrolysis as well as acid or base catalysis. However, organometallic type catalysts provide the highest degree of selectivity in the production of α−olefins.[1] Most recently, interest has been directed toward transition metal based catalysts with a bidentate chelating ligand, X−Y. Thus, Keim and co-workers have developed a number of nickel-containing catalysts[2] with X−Y = O−O and P−O, respectively. Similar catalysts with S−S ligands were reported by Brown and Masters.[3] Active titanium-based catalyst have also been developed by Krzywicki.[4]

There has been a number of theoretical studies on ethylene polymerization. The more recent studies[5] have concentrated on olefin polymerization catalyzed by Kaminsky type metallocenes of early transition metals.[6] The emphasis in all theoretical polymerization studies have been on the chain-growing step whereas the much slower chain terminating processes have received much less attention. Ethylene dimerization and oligomerization have by contrast not been the subject of recent *ab initio* studies. In oligomerization chain growth and chain termination take place at comparable rates. However, it is not clear from the experimental or theoretical studies carried out to date why metallocenes of early transition metals favor polymerization whereas nickel based catalysts with a bidentate chelating ligand, X−Y, favor oligomerization.

The mechanism for oligomerization catalyzed by transition metal complexes is not yet fully established. Keim[2] has proposed a mechanism for his nickel-based systems in which a nickel hydride species is assumed to be the actual catalyst. The cycle proposed by Keim is shown in Scheme 1 for the dimerization of ethylene with acetylacetonate (acac) nickel hydride as the catalyst. It is assumed that (acac)Ni−H is formed from bis(cyclooctadiene-1,5)nickel according to the process in eq 1.

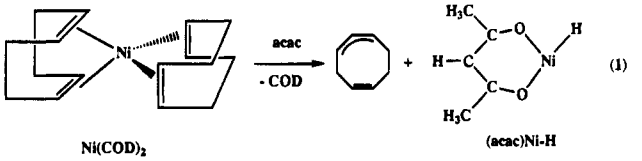


Ni(COD)$_2$ (acac)Ni-H (1)

The first step, **S1**, in the cycle represents the formation of an ethylene $\pi$-complex, **II**, followed by the insertion, **S2**, of $C_2H_4$ into the nickel-hydride bond to form the ethyl derivative, **III**, Scheme 1. The sequence **S1** + **S2** resembles the insertion steps

† Novacor Research & Technology Corporation.
‡ University of Calgary.
⊗ Abstract published in *Advance ACS Abstracts,* October 1, 1994.

(1) Keim, W.; Behr, A.; Roper, M. In *Comprehensive Organometallic Chemistry*; Wilkinson, G., Stone, F. G. A., Abel, E. W., Eds.; Pergamon: New York, 1982; Chapter 52, p 371.
(2) (a) Keim, W. *Angew. Chem. Int. Ed. Engl.* **1990**, *29*, 235. (b) Keim,W.; Hoffmann, B.; Lodewick, R.; Peuckert, M.; Fleischhauer, J.; Meier, U.; Schmitt, G. *J. Mol. Catal.* **1979**, *6*, 79. (c) Keim,W.; Behr, A.; Kraus, G. *J. Organomet. Chem.* **1983**, *251*, 377. (d) Behr, A.; Falbe, V.; Freudenberg, U.; Keim,W. *Isr. J. Chem.* **1986**, *27*, 277.
(3) (a) Brown, S. J.; Masters, A. F. *J. Organomet. Chem.* **1989**, *367*, 371. (b) Abcywickrema, R.; Bennett, M. A.; Cavell, K. J.; Kony, M.; Masters, A. F.; Webb, A. G. *J. Chem. Soc. Dalton Trans.* **1993**, 59.
(4) (a) Krzywicki, A.; Johnstone, K. In *Progress in Catalysis*; Smith, K. J.; Sanford E. C., Eds.; Elsevier: Amsterdam 1992. (b) Krzywicki, A.; Jurric, P. Can. Pat. 1298829, April 14, 1992.
(5) (a) Fujimoto, H.; Yamasaki, T.; Mizutani, H.; Koga, N. *J. Am. Chem. Soc.* **1985**, *107*, 6157. (b) Lolly, C. A.; Marynick, D. S. *J. Am. Chem. Soc.* **1989**, *111*, 7968. (c) Castonguay, L. A.; Pappe, A. K. *J. Am. Chem. Soc.* **1992**, *114*, 5832. (d) Kawamura-Kuribayashi, H.; Koga, N.; Morokuma, K. *J. Am. Chem. Soc.* **1992**, *114*, 2359. (e) Kawamura-Kuribayashi, H.; Koga, N.; Morokuma, K. *J. Am. Chem. Soc.* **1992**, *114*, 8687. (f) Woo, T. K.; Fan, L.; Ziegler, T. Organometallics, submitted for publication.
(6) Sinn, H.; Kaminsky, W.; Vollmer, H.; Woldt, R. *Angew. Chem., Int. Ed. Engl.* **1980**, *19*, 390.

0020-1669/94/1333-5287$04.50/0 

**Scheme 1**

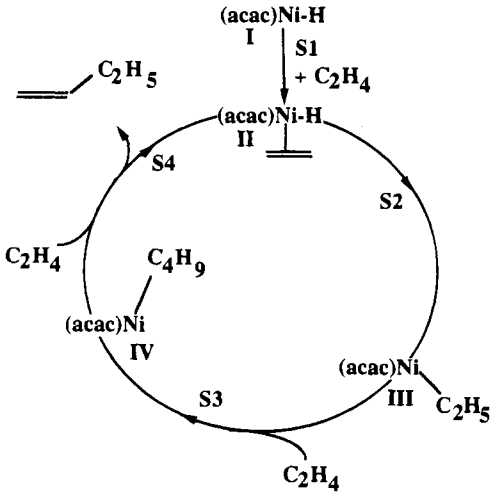


proposed by Cossee[7] in his mechanism for olefin polymerization. The next step, **S3**, gives rise to a new ethylene insertion, and the formation of the butyl complex, **IV**. The cycle is completed when the butyl complex, **IV**, reacts in **S4** with another ethylene to form the 1-butene product and the regenerated $\pi$-complex **II**.

The present investigation has several objectives. We want in the first place to characterize the molecular and electronic structure of the catalytic hydride **I**. Some evidence for the existence of **I** during the oligomerization process has been provided.[8] However, unsaturated three-coordinated nickel hydrides such as **I** have not been isolated and characterized. The thermochemistry of steps **S1** and **S2** as well as the structures of the ethylene $\pi$-complex **II** and the insertion product **III** will also be examined. We shall further assess the thermochemistry for the terminating sequence **S4** in which 1-butene is formed and the catalytic species **II** regenerated according to

$$\mathbf{VI} + C_2H_4 \rightarrow C_4H_8 + \mathbf{II} \qquad (2)$$

We shall finally try to assess the thermochemistry of the process in eq 2 relative to the reaction enthalpy of a regular insertion step in which **IV** reacts with ethylene to form the hexyl derivative (acac)Ni$-C_6H_{13}$ according to

$$\mathbf{IV} + C_2H_4 \rightarrow (\text{acac})\text{Ni}-C_6H_{13} \qquad (3)$$

The emphasis in the present investigation is clearly on the thermochemistry of the processes in Scheme 1 as well as the structure of some of the species involved in dimerization of ethylene. We have not been able to carry out detailed reaction path calculations on the insertion processes of Scheme 1. Thus, only rough estimates of the activation barriers can be provided for these reactions. An actual transition state structure will be provided for the termination step, **S4**, in which 1-butene is displaced from the butyl complex **IV**.

## 2. Computational Details

Density Functional Theory[9] (DFT) has been widely recognized as a powerful alternative computational method to traditional *ab initio* schemes, particularly in studies of transition metal complexes where large size basis sets and an explicit treatment of electron correlation are required. The local spin density approximation[10] (LDA) is the most frequently applied approach within the families of approximate DFT schemes. It has been used extensively in studies on solids and molecules. Most properties obtained by the LDA scheme are in better agreement with experiment than data estimated by *ab initio* calculations at the Hartree–Fock level.[9a] However, bond energies are usually overestimated by LDA. Thus, gradient or nonlocal corrections[11] have been introduced to rectify shortcomings in the LDA approximation. The nonlocal corrections can be introduced as a perturbation or incorporated in a fully variational calculation. In the perturbative approach the nonlocal energy functional is evaluated based on the LDA electronic density while in the variational approach the electronic density itself is determined by optimizing the gradient corrected energy. The variational procedure is computationally more demanding than the perturbative approach by a factor of 2–3. We have shown in previous studies[12] that the density change induced by nonlocal correction is minor and that the two approaches lead to similar results for most of the molecular properties that have been studied.

All calculations were carried out by the AMOL program due to Baerends[13] et al. In the present investigation the molecular geometries were all optimized based on the LDA approximation in the parametrization due to Vosko[14] *et al.* Single-point energy evaluations were then carried out with Becke's[11b] nonlocal exchange correction and Perdew's[11c] nonlocal correlation correction. The basis[15] set used for the 3s, 3p, 3d, and 4s valence shells on nickel was of triple-$\zeta$ quality and augmented by three 4p Slater-type-orbitals (STO). The triple-$\zeta$ basis set used for the 2s and 2p valence orbitals on fluorine was augmented by two 3d polarization functions. A double-$\zeta$ basis set was applied for the 2s and 2p shells of oxygen and carbon as well as the 1s shell of hydrogen. An additional 3d STO was added to oxygen and carbon whereas hydrogen was given a single 2p STO. All inner shell orbitals were kept frozen[13] in the variational calculations. A set of auxiliary[16] s, p, d, f, and g type of STOs centered on the different atoms was used to fit the electronic density. The numerical integrations were carried out according to the scheme[17] proposed by te Velde *et al.* Geometries were optimized on the basis of the scheme implemented by Versluis and Ziegler.[18]

## 3. Results and Discussion

**Structure of the Hydride Catalyst.** The chelated nickel hydride **I** is assumed to be the active species in the olefin dimerization cycle depicted in Scheme 1. However, no experimental data are available on the electronic and molecular structure of **I**. We have investigated three possible geometries of a model hydride in which the methyl groups on the acac ligand of **I** have been replaced by hydrogens to produce the propanedial anion.

The hydride of highest symmetry, **1a**, has the Ni–H bond in the chelate plane, and the Ni–H bond vector bisecting the O–Ni–O angle. Conformation **1a** is of $C_{2v}$ point group

(7) Cossee, P. *J. Catal.* **1964**, *3*, 80.
(8) (a) Müller, U.; Keim, K.; Krüger, C.; Betz, P. *Angew. Chem., Int. Ed. Engl.* **1989**, *28*, 1011. (b) Jolly, P. W.; Milke, G. *The Organic Chemistry of Nickel*; Academic Press: New York, 1975, Vol. 2. (c) Bogdnanovic, B. *Adv. Organomet. Chem.* **1979**, *17*, 105.
(9) (a) Ziegler, T. *Chem. Rev.* **1991**, *91*, 651. (b) Parr, R. G.; Yang, W. *Density Functional Theory of Atoms and Molecules*; Oxford University Press: New York, 1989.
(10) Dahl, J. P.; Avery, J., Eds. *Local Density Approximations in Quantum Chemistry and Solid State Physics*; Plenum: New York, 1984.
(11) (a) Hu, C. D.; Langreth, D. C. *Phys. Rev.* **1986**, *B33* 943. (b) Becke, A. D. *Phys. Rev.* **1988**, *A38*, 3098. (c) Perdew, J. P. *Phys. Rev.* **1986**, *B33*, 8822. Also see the erratum: *Phys. Rev.* **1986**, *B34*, 7046. (d) Wilson, L. C.; Levy, M. *Phys. Rev.* **1990**, B41, 12930.
(12) (a) Fan, L.; Ziegler, T. *J. Chem. Phys.* **1991**, *94*, 6057. (b) Fan, L.; Ziegler, T. *J. Chem. Phys.* **1991**, *95*, 7401. (c) Fan, L.; Ziegler. T. *J. Chem. Phys.* **1992**, *96*, 9005. (d) Fan, L.; Ziegler, T. *J. Phys. Chem.* **1992**, *96*, 6937.
(13) Baerends, E. J.; Ellis, D. E.; Ros, P. *Chem. Phys.* **1973**, *2*, 41.
(14) Vosko, S. H.; Wilk, L.; Nusair, M. *Can. J. Phys.* **1980**, *58*, 1200.
(15) (a) Snijders, G. J.; Baerends, E. J.; Vernooijs, P. At. Nucl. Data Tables **1982**, *26*, 483. (b) Vernooijs, P.; Snijders, G. J.; Baerends, E. J. *Slater Type Basis Functions for the whole Periodic System*; Internal Report; Free University of Amsterdam: Amsterdam, 1981.
(16) Krijn, J.; Baerends, E. J. *Fit functions in the HFS-method*; Internal Report (in Dutch), Free University: Amsterdam, 1984.
(17) Boerrigter, P. M.; te Velde, G.; Baerends, E. J. *Int. J. Quantum Chem.* **1988**, *33*, 87.
(18) Versluis, L.; Ziegler, T. *J. Chem. Phys.* **1988**, *88*, 322.

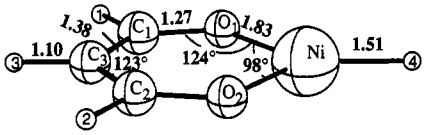


**8.1 kcal/mol**

**1a**

symmetry, and it has a $^3B_2$ triplet ground state corresponding to the $(1a_2)^2(1b_1)^2(1a_1)^2\ (2a_1)^1(1b_2)^1$ electron configuration, Figure 1. The $d^8$ hydride has two unpaired electrons placed in the closely spaced antibonding orbitals $2a_1$ and $1b_2$ made up of respectively $d_{x^2-y^2}$ and $d_{xy}$ on nickel.

A distortion of the Ni−H bond in **1a** out of the chelate plane leads to **1b** of $C_s$ symmetry. This conformation has a $^3A''$ triplet ground state with the electron configuration $(1a'')^2(1a')^2(2a')^2$-

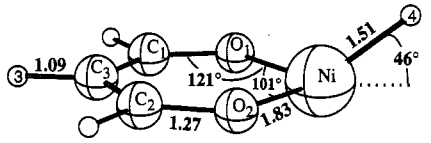


**2.8 kcal/mol**

**1b**

$(3a')^1(2a'')^1$, Figure 1. The distortion of the Ni−H bond out of the chelate plane will stabilize the $d_{x^2-y^2}$-based orbital $2a_1$ of **1a** as the antibonding interaction with hydrogen is removed, leading to the nonbonding $d_{x^2-y^2}$-based orbital 2a′ of **1b**, Figure 1. However, the distortion will at the same time destabilize $1b_1$ ($d_{xz}$) which evolves into 3a′ of **1b**. This orbital has an antibonding interaction between $d_{xz}$ and $1s_H$. Thus **1b**, like **1a**, has two closely spaced antibonding d-based orbitals and adopts a high-spin configuration. Conformation **1b** is related to a tetrahedral $d^8$ nickel complex with one ligand removed. Most tetrahedral $d^8$ nickel complexes have a triplet ground state. We calculate **1b** to be more stable than **1a** by 5.3 kcal/mol.

The most stable hydride conformation is **1c**. It is related to **1a** by an in-plane distortion of the N−H bond from the $C_2$ symmetry axis by 43°. This distortion will stabilize $2a_1$ of **1a** just as in **1b**, but without introducing another strongly anti-

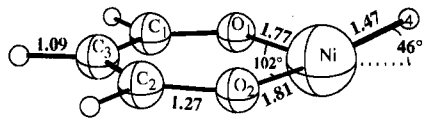


**0 kcal/mol**

**1c**

bonding orbital, Figure 1. In **1c** there is only one antibonding orbital, 3a′, and **1c** adopts a low spin $^1A'$ ground state corresponding to the $(1a'')^2(2a'')^2(1a')^2(2a')^2$ electron configuration. The conformation **1c** is related to a square planar geometry with one ligand missing, and square planar $d^8$ nickel complexes are low spin. Conformation **1c** is lower in energy than **1a** by 8.2 kcal/mol.

The chelate ring structures are quite similar in the three conformations. The only noticeable difference is the Ni−O distances which are slightly shorter in **1c** than in **1a** and **1b**. The nickel and hydrogen atoms are also bonded more tightly in **1c** with a N−H bond length of 1.468 Å which is 0.04 Å shorter than in **1a** and **1b**. The stronger Ni−H and Ni-O bonds in **1c** reflect the fact that no Ni−ligand antibonding orbital is occupied in this species, Figure 1.

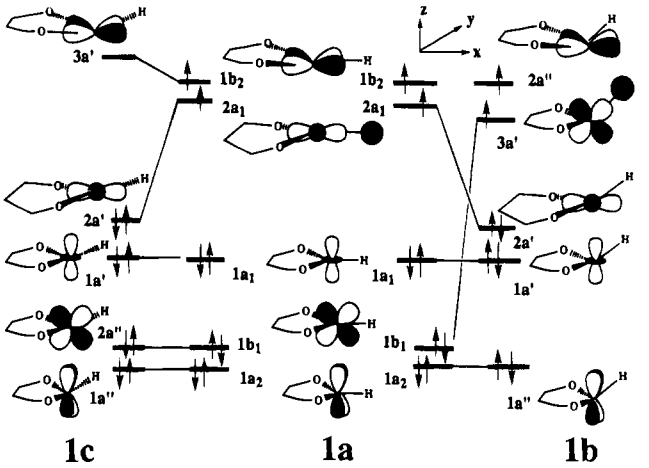


**Figure 1.** Diagram correlating d-based orbitals of the metal hydrides **1a**, **1b**, and **1c**.

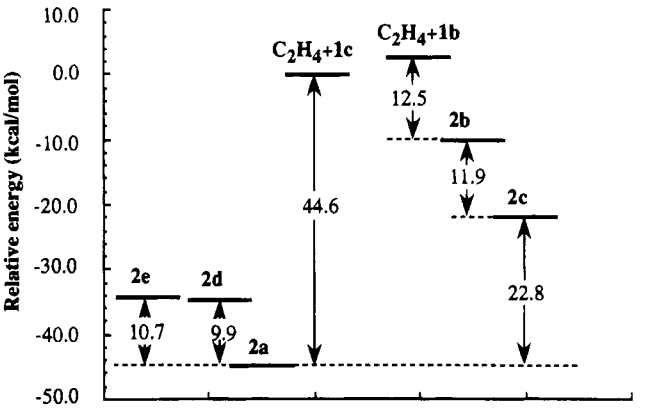


**Figure 2.** Energetics of ethylene insertion into Ni−H bond of **1c**.

**First Insertion of Ethylene**. It follows from Scheme 1. that the first step, **S1**, in the dimerization of ethylene involves the formation of an ethylene $\pi$-complex, **II**, followed by the insertion, **S2**, of $C_2H_4$ into the nickel−hydride bond to form the ethyl derivative, **III**. The ethylene molecule can approach the hydride, **1c**, in the chelate plane or perpendicular to the chelate plane.

Starting with the first approach, we have tried to optimize a $\pi$-complex, **II**, with ethylene in the chelate plane leading to a 16-electron square-planar complex. Different starting geometries lead invariably directly to an ethyl complex, **III**, rather than the $\pi$-complex, **II**. It seems as if no local minimum exists for an in-plane $\pi$-complex, **II**, on the potential energy surface.

The stable square planar ethyl structure with all degrees of freedom optimized is depicted as **2a**. One of the hydrogens, $H_8$ , on the ethyl group in **2a** exhibits a strong $\beta$-agostic

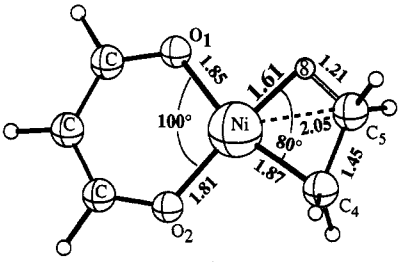


**0 kcal/mol**

**2a**

interaction with the nickel atom. The Ni−$H_8$ distance of 1.61 Å is only 0.14 Å longer than in the free hydride, **1c**. At the

same time the $H_8-C_5$ distance has been stretched to 1.21 Å which is 0.1 Å longer than an ordinary C−H bond in ethylene. The $C_4-C_5$ distance on the ethyl group of 1.45 Å is further seen to be shorter than an ordinary carbon−carbon single bond of 1.54 Å, indicative of some double bond character. The strong agostic interaction involves a donation of charge from the $C_5-H_8$ $\sigma$-bonding orbital to the empty 3a′ orbital on **1c**, Figure 1. In **2a** the Ni−H bond has been maintained while ethylene has formed two new bonds to nickel and hydrogen, respectively. It is thus not surprising that the reaction between **1a** and ethylene is highly exothermic with a reaction enthalpy of 44.6 kcal/mol, Figure 2 .

We have been able to locate a tetrahedral $\pi$-complex, **2b**, with an open-shell triplet ground state that could be reached from a perpendicular approach of ethylene toward **1c**. The

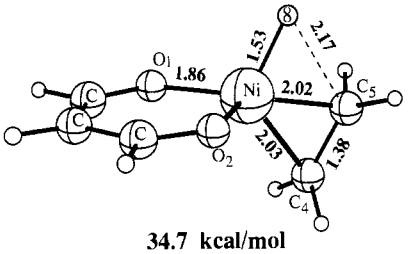


**34.7 kcal/mol**

**2b**

structure **2b** is a typical $\pi$-complex in which the two carbon atoms of ethylene are at similar distances to nickel with Ni−$C_4$ = 2.03 Å and Ni−$C_5$ = 2.02 Å, respectively. In addition, both bonds are longer than the nickel−ethyl single bond in **2a** with Ni−$C_4$ = 1.86. The ethylene double bond has as expected been elongated from 1.34 to 1.38 Å due to the donation of charge from the metal center to the $\pi^*$ olefin orbital. Finally, the Ni−$H_8$ bond distance of 1.53 Å is only slightly longer than the Ni−H distance of 1.51 Å in the high-spin tetrahedral based hydride **1b**. The $\pi$ complexation energy for the process **1c** + $C_2H_4$ → **2b** was calculated to be 9.7 kcal/mol. The $\pi$-complex **2b** is 12.5 kcal/mol more stable than free **1b** and $C_2H_4$, Figure 2. However, **2b** is 34.7 kcal/mol above **2a** in energy.

It was also possible to optimize an ethyl complex **2c** with a triplet ground state. This complex can be considered as the product due to a further perpendicular approach of ethylene from

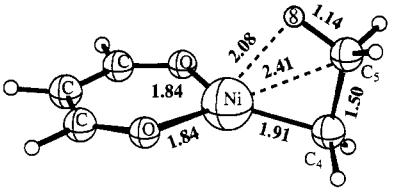


**22.8 kcal/mol**

**2c**

**2b** toward the metal center leading to an insertion of $C_2H_4$ into the Ni−H bond. We note a modest $\beta$-agostic interaction with a stretch of the $C_5-H_8$ bond to 1.14 Å and a Ni−$H_8$ contact distance of 2.09 Å, which is much longer than the normal Ni−H bond distance of 1.5 Å. We can consider **2c** as the ethyl analogues to the high-spin tetrahedral based hydride **1b**. The insertion process **2b** → **2c** is calculated to be exothermic by 11.9 kcal/mol, Figure 2.

Figure 2 summarizes the energetics for the species involved in the insertion of $C_2H_4$ into the Ni−H bond of **1c** for the in-plane as well as perpendicular approach. The species, **2a**, formed by an in-plane approach of $C_2H_4$ toward **1c** is seen to be more stable than the high spin ethyl complex, **2c**, from the perpendicular approach by 22.8 kcal/mol, Figure 2. Essentially, **2a** is much more stable than **2c** on account of the stronger $\beta$-agostic interaction and the preference of a low-spin square planar conformation over a high-spin tetrahedral structure, **1c** versus **1b**.

It is possible to estimate the strength of the $\beta$-agostic interaction in **2a** by looking at low spin square planar ethyl isomers of **2a** in which this interaction is absent. We have looked at the two isomers **2d** and **2e**. In **2d** the methyl group

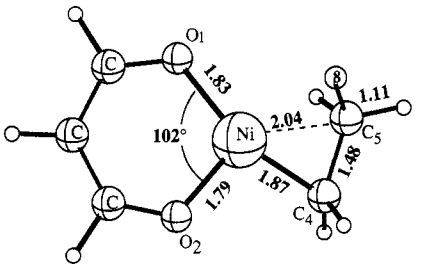


**9.9 kcal/mol**

**2d**

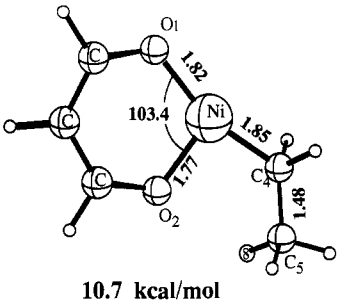


**10.7 kcal/mol**

**2e**

has been rotated by 60° around the $C_4-C_5$ bond axis. The Ni−$H_8$ distance is now elongated to 2.07 Å compared to 1.61 Å in **2a**. It follows from Figure 2 that **2d** is 9.9 kcal/mol above **2a**, Figure 2. This energy gap can be considered approximately as the agostic $\beta$-hydrogen interaction energy of **2a**.

Structure **2e** corresponds to a conformation in which the ethyl group of **2d** has been rotated by 180° around the Ni−$C_4$ bond vector. Conformation **2e** is analogous to the catalyst **1c**, which has an empty coordination site for an incoming ethylene. The energy of **2e** is only 0.8 kcal/mol higher than that of **2d** and 10.7 kcal/mol above **2a**, Figure 2.

Our study on the insertion of ethylene into the Ni−H bond of **I** has concentrated on the thermochemical aspects. We have not actually carried out calculations on the reaction paths along the in-plane and perpendicular approaches. However, the preference of the chelated nickel center for a square planer low-spin coordination chemistry seems to indicate that in in-plane approach is the most favorable. Certainly, the product **2a** from the in-plane approach is thermodynamically more stable than the product, **2c**, from the perpendicular approach.

**The Second Insertion of Ethylene.** Our study on the insertion of ethylene into the Ni-ethyl bond, **S3**, will also focus on the thermodynamical aspects. We shall in addition restrict our investigations to species that conceivably could be of importance for the in-plane approach.

Figure 4 gives the two possible in-plane paths, **A1** and **A2**, of ethylene toward the ethyl complex **III**, with **III** in its most stable conformation, **2a**. The first path, **A1**, has ethylene entering directly toward the agostic $\beta$-hydrogen, $H_8$, whereas ethylene is approaching from the back side toward the $\beta$-carbon

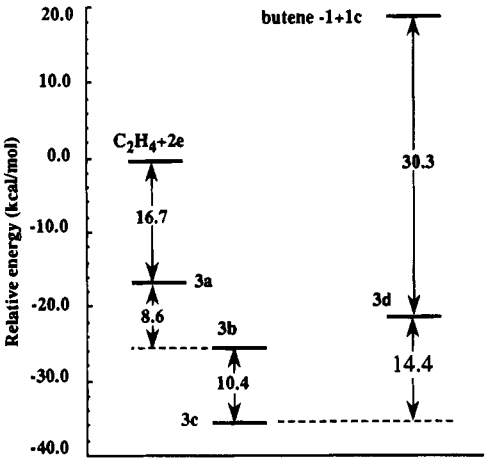


**Figure 3.** Energetics of ethylene insertion into Ni−ethyl bond of **2e**.

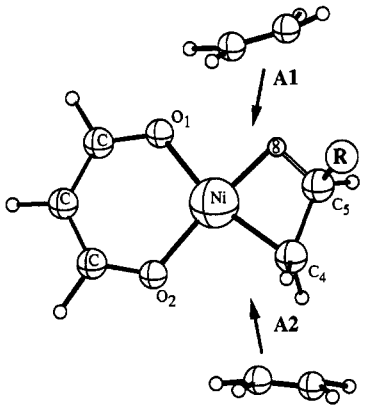


**Figure 4.** Different in-plane paths for the insertion of ethylene into the Ni−ethyl bond of **2a**.

in **A2**. In both paths one expects the Ni−$H_8$ agostic bond to break as the insertion process proceeds. One could alternatively imagine a rearrangement of **2a** to **2d** or **2e** in which the Ni−$H_8$ agostic bond is broken followed by an attack of ethylene.

We have optimized the species **3a** without any symmetry constraints. This structure can be characterise as a genuine $\pi$-complex, and it is possible to imagine the formation of **3a**

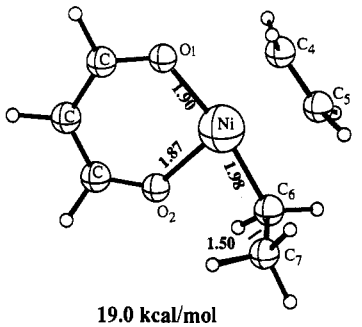


19.0 kcal/mol

**3a**

from each of the approaches discussed above. The coordination of $C_2H_4$ in **3a** leads to two relatively short Ni-C(ethylene) bonds of 1.98 Å and a slight elongation of the ethylene double bond by 0.02 Å to $R(C_4-C_5)$ = 1.36 Å. The nickel-ethyl bond has at the same time stretched from 1.85 Å in **2e** to $R(Ni-C_6)$ = 1.98 Å in **3a**. The distance in **3a** between the ethylene carbon $C_5$ and the ethyl carbon $C_6$ of 2.39 Å is still too long for any C−C bond formation.

The formation of **3a** from the coordination of ethylene to **2e** is exothermic by 16.7 kcal/mol, as shown in Figure 3. This exothermicity exceeds the energy (10.7 kcal/mol) required to transform the most stable ethyl complex **2a** into **2e** by removing the strong $\beta$-agostic Ni−$H_8$ interaction.The formation of **3a** from **2a** and ethylene is thus exothermic by 6.0 kcal/mol.

The optimized structure **3b** can be viewed as the direct product from the insertion of ethylene into the Ni−ethyl bond starting from **3a**. Conformation **3b** is a butyl complex with a

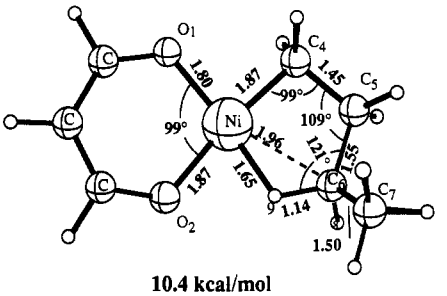


10.4 kcal/mol

**3b**

$\gamma$-agostic interaction. The five-membered ring in **3b** is nearly planar. As a consequence, two of the angles at the ethyl carbons, i.e. $\theta(C_5C_4Ni)$ and $\theta(H_9C_6C_5)$, are distorted from the $sp^3$ value of 109.5° to 99° and 121°, respectively . However, the stress in the ring is compensated for by the $\gamma$-agostic Ni−H bond with a distance of R(Ni−H) = 1.65 Å.

The process **3a** → **3b** is exothermic by 8.6 kcal/mol, Figure 3, and the total reaction enthalpy for the process **2e** + $C_2H_4$ → **3b** is thus −25.3 kcal/mol, compared to −44.6 kcal/mol for the first ethylene insertion , **1c** + $C_2H_4$ → **2a**. The first insertion is more favorable since we form two new bonds, Ni−C and C−C, while retaining the Ni−H interaction. In the second insertion, only a C−C link is form while retaining the Ni−H interaction.

Conformation **3b** can isomerize to the more stable butyl compound **3c** with a $\beta$-agostic Ni−H bond by a rotation around the $C_4-C_5$ axis. The complex **3c** is in many ways similar to

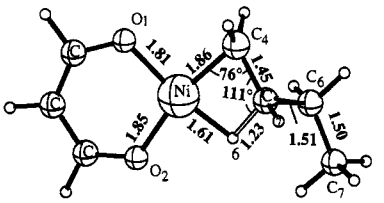


0.0 kcal/mol

**3c**

**2a** with a Ni−C bond distance of $R(Ni-C_4)$ = 1.86 Å, a C−C distance of $R(C_4-C_5)$ = 1.45 Å, a Ni−H bond of 1.61 Å, and a C−C−Ni bond angle of $\theta(C_5C_4Ni)$ = 76°. The Ni−H $\beta$-agostic interaction in **3c** is likely stronger than the $\gamma$-agostic interaction in **3b** since **3c** has a shorter Ni−H bond as well as a longer C−H distance for the C−H bond involved in the agostic interaction. The less strained butyl chain and stronger agostic interaction in **3c** makes this conformation more stable than **3b** by 10.4 kcal/mol, Figure 3. Of all optimized butyl structures **3c** had the lowest energy just as its analogue **2a** represents the most stable conformation among the ethyl complexes. The second insertion step, **2a** + $C_2H_4$ → **3c**, from the most stable ethyl complex, **2a**, to the most stable butyl complex, **3c**, is exothermic by 25 kcal/mol, and we expect a similar exothermecity for each subsequent insertion step.

We have finally studied an open conformation, **3d**, in which the nickel center and the α-carbon are exposed, and readily susceptible to the next insertion step. The butyl structure **3d**

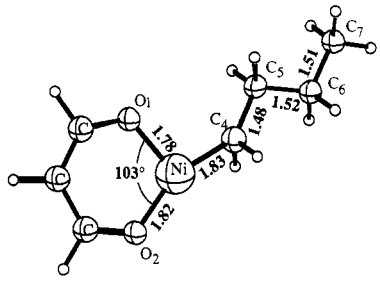


14.4 kcal/mol

**3d**

can be reached from **3c** by a rotation around the Ni−$C_4$ bond and is in many ways similar to the ethyl complex **2e**. The rotation around the Ni−$C_4$ axis will break the agostic Ni−$H_8$ bond, and we calculate the **3c** to **3d** rearrangement to cost 14.4 kcal/mol in energy, Figure 3. It is not required that **3c** rearrange to **3d** prior to the next insertion; the rearrangement can take place in concert with the olefin approach. We expect, however, some barrier for each insertion cycle as the agostic interaction is broken up to make space for another incoming olefin.

**Chain Termination Mechanism.** The discussion above has been concerned with chain growth leading to oligomers. We have concluded that the insertion step **S3** of Scheme 1 is exothermic with an estimated reaction enthalpy of −25 kcal/mol. However, the insertion is likely to exhibit a barrier in the initial stages when the most stable conformation, **2a**, of the ethyl complex **III** has to rearrange prior to or in concert with the ethylene approaches.

The next step in Scheme 1 involves the reaction between the ethyl species **III** and ethylene, **S4**. This reaction can lead to another insertion according to eq 3 or to the formation of 1-butene following eq 2.

We have not studied the insertion process of eq 3 in detail. It is assumed that this reaction is very similar to the insertion process of **S3** with roughly the same reaction enthalpy of −25 kcal/mol and a barrier associated with the rearrangement of **3c** to **3d** so as to expose the vacant coordinate site on Ni and allow for an unhindered attack by ethylene on the α-carbon, $C_4$.

We shall now turn to the chain terminating step of eq 2 which is shown in Scheme 1 as **S4**. This step releases 1-butene and ensures that ethylene is oligomerized rather than polymerized. We calculate the terminating process of eq 2 to be nearly thermoneutral with a reaction heat of 0.1 kcal/mol.

One possible mechanism for **S4** involves a β-hydrogen elimination of **IV** to generate the hydride **I** and the product 1-butene according to eq 4. The hydride **I** can then react with

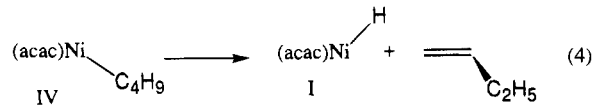


(4)

ethylene to continue the cycle in Scheme 1. We find that the β-hydrogen elimination step of eq 4 is highly endothermic with a reaction enthalpy for the process

$$\mathbf{3c} \rightarrow \mathbf{1c} + \text{1-butene} \qquad (5)$$

of 44.7 kcal/mol, Figure 3. Thus, it is not likely that β-hydrogen elimination as illustrated in eq 4 is an integral part of **S4**.

Square planar low-spin $d^0$ nickel complexes are known to undergo substitution reactions via five coordinated intermediates or transition states. It is thus tempting to suggest an alternative mechanism for **S4** according to Scheme 2. The first step here is the formation of the π-adduct **4a** between $C_2H_4$ and **3c**. The

**Scheme 2**

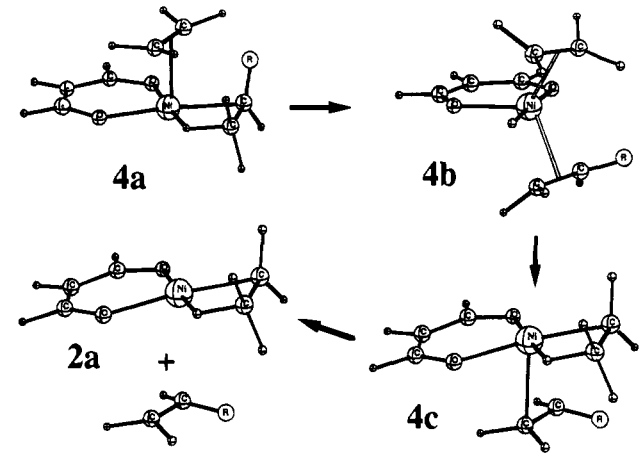


next step involves the displacement (substitution) of 1-butene by ethylene via the transition state **4b** and the π-adduct **4c**. In the transition state **4b**, 1-butene and ethylene are π-coordinated symmetrically to nickel on each side of the chelate coordination plane of **1c**. The process in Scheme 2 is a β-hydride elimination induced by an incoming olefin. The process is aided by the fact that both the eliminated olefin and the incoming olefin can π-complex to the metal.

We have studied the reaction in Scheme 2 for the degenerate process of eq 6a, where R of Scheme 2 is hydrogen. For step **S4** of Scheme 1 we have R = ethyl. A transition state of $C_s$

$$\mathbf{2a} + C_2H_4 \rightarrow \mathbf{2a} + C_2H_4 \qquad (6a)$$

symmetry was optimized as **4d** for the process in eq 6a. The structure **4d** has one imaginary frequency of 861.4*i* $cm^{-1}$. The transition state **4d** can best be characterized as a metal hydride with two π-complexed olefins. The Ni−$H_1$ distance is 1.51 Å whereas the shortest C−$H_1$ distance is 1.67 Å. We can best characterized the process in eq 6a as a substitution-induced β-hydride elimination where both the incoming and outgoing olefin is coordinated to the nickel in the transition state. The optimized transition state was calculated to be 16 kcal/mol above the reactants **2a** + $C_2H_4$. We have also optimized the structure for the π-adduct **4c**. It has an energy which is 1 kcal/mol below that of the reactants **2a** + $C_2H_4$.

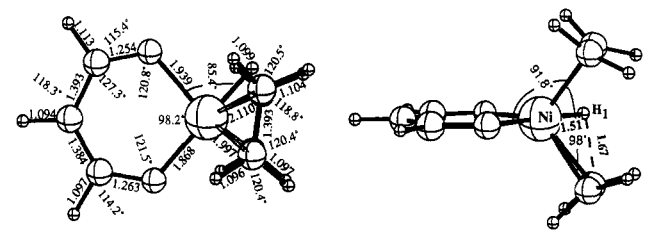


**4d**

The internal barrier for the elimination step according to Scheme 2 is calculated to be 17 kcal/mol. A barrier of that size is reasonable in view of the fact that ethylene dimerization takes place at 40 °C. We propose that the mechanism given in Scheme 2 with R = $C_2H_5$ also is viable for the process of eq 6b, where 1-butene is eliminated and the ethyl species **2a** regenerated.

$$\mathbf{3c} + C_2H_4 \rightarrow C_4H_8 + \mathbf{2a} \qquad (6b)$$

**Scheme 3**

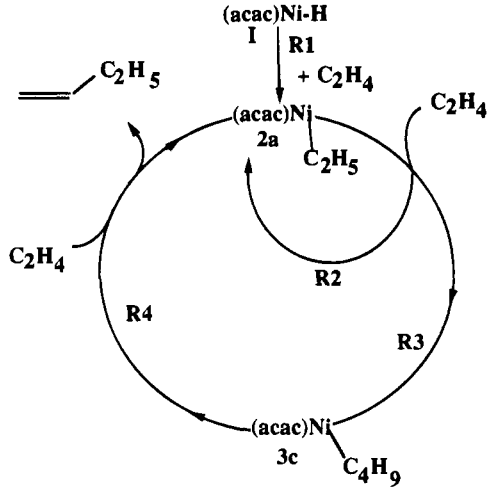


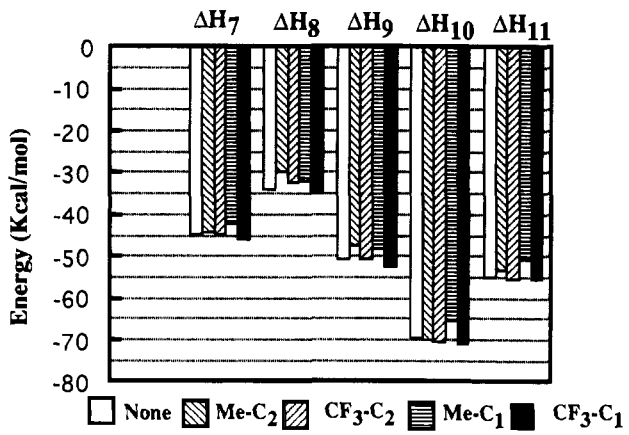


**Figure 5.** The calculated reaction enthalpies $\Delta H_n$ ($n$ = 7−11) for the processes (7−11) defined in text.

Our investigation of the elimination mechanism in Scheme 2 and the insertion steps in Scheme 1 has lead us to proposed the modified mechanism for ethylene dimerization given in Scheme 3.

The species regenerated in the oligomerization cycle of Scheme 3 is the stable ethyl complex **2a**. The ethyl complex **2a** might initially be formed from ethylene and the hydride **1c** in the step **R1**. The first step in the cycle is the reaction of **2a** with ethylene. It can lead to the degenerate process **R2** in which **2a** is regenerated according to eq 6a. Alternatively, ethylene might insert into the Ni−ethyl bond and form the butyl complex **3c** according to **R3**. The second step in the cycle involves the reaction with ethylene and the butyl complex **3c**, eq 6b. This reaction can produce 1-butene and regenerate the ethyl complex **2a** according to the substitution mechanism of Scheme 2. Alternatively, ethylene might insert into the Ni-butyl bond to form the Ni−hexyl complex according to eq 3. In that case higher oligomers will be formed.

**Modifications of the Chelate Ligand.** The actual catalysts for ethylene dimerization have $CF_3$ groups attached to the chelate ring. It is not clear whether the $CF_3$ substituents simply improve the soluability and thermal stability of the catalyst or whether the electron-withdrawing $CF_3$ groups in fact have a direct influence on the thermochemistry of the steps in Schemes 1 and 3.

We have looked in some details at the way in which substituents on the $C_1$ and $C_2$ carbons of the chelate ligand might influence the thermochemistry of the steps in Scheme 1 and Scheme 3. Four substitutions were considered, and they are shown for the hydride **1c** in **5a−d**. The substitutions involve

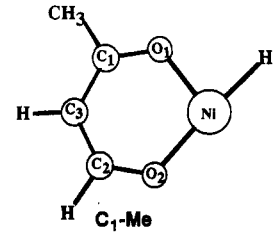


**5a**

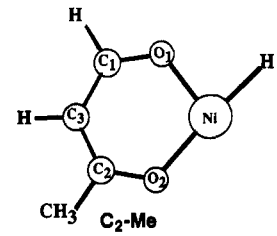


**5b**

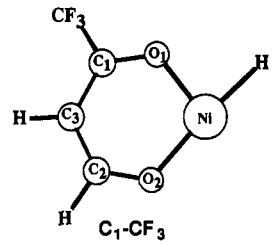


**5c**

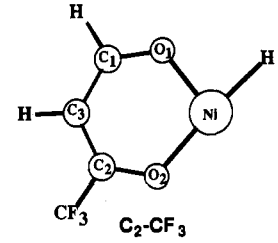


**5d**

replacing hydrogen with methyl, $C_1$−Me (**5a**) and $C_2$−Me (**5b**), or $CF_3$ groups, $C_1$−$CF_3$ (**5c**) and $C_2$−$CF_3$ (**5d**), in the $C_1$ and $C_2$ positions. A full optimization of the structures **5a−d** revealed hardly any change in the chelate ring structure. The most notable perturbation was in the species **5c** and **5d** with the electron-withdrawing $CF_3$ substituent. Here the Ni−H distance is shortened by 0.005 Å compared to **1c**.

We have reinvestigated the thermochemistry for the processes

$$\mathbf{1c'} + 2C_2H_4 \rightarrow \mathbf{2a'} + C_2H_4 + \Delta H_7 \quad (7)$$

$$\rightarrow \mathbf{2e'} + C_2H_4 + \Delta H_8 \quad (8)$$

$$\rightarrow \mathbf{3a'} + \Delta H_9 \quad (9)$$

$$\rightarrow \mathbf{3c'} + \Delta H_{10} \quad (10)$$

$$\rightarrow \mathbf{3d'} + \Delta H_{11} \quad (11)$$

with the Me−$C_1$, Me−$C_2$, $CF_3$−$C_1$, and $CF_3$−$C_2$ substitutions. The species **2a'**, **2e'**, **3a'**, **3c'**, and **3d'** were generated from the parent molecules **2a**, **2e**, **3a**, **3c**, and **3d** by replacing a hydrogen with a $CH_3$ or $CF_3$ group. The structures of the $C_n$−$CF_3$ and $C_n$−$CH_3$ moieties ($n$ = 1, 2) in the substituted species were taken from the optimized structures of **5a−d**. The remaining part of the structure for the substituted species was taken from the parent molecules.

Figure 5 displays $\Delta H_n$ ($n$ = 7−11) for the four different substitutions as well as the parent systems. It is clear from Figure 5 that the influence of substitution on $\Delta H_n$ ($n$ = 7−11) is marginal. For the $CF_3$-substituted species the processes become more exothermic by 2−3 kcal/mol compared to the reactions involving the parent molecules. For the $CH_3$ substituted species a corresponding drop in exothermicity of 2−3 kcal/mol is observed.

Our calculations would indicate that $CF_3$ substitution on the chelate ring has little direct influence on the thermochemistry of the steps in Schemes 1 and 3. However, fluorosubstitutions may add thermal stability to the catalytic system and make it more soluble.

## 4. Concluding Remarks

The main objective of this investigation has been to study the structure and relative stability of species involved in the

mechanism proposed by Keim et al.[1] for the dimerization of ethylene according to Scheme 1.

Three conformations have been studied for the hydride **I**, which is the pre-catalyst according to Scheme 1. We have found that the chelated nickel center prefers a low-spin conformation, **1c**, with a square planar structure where one site is vacated cis to hydrogen. The initial insertion of ethylene into the Ni−H bond, **S1** + **S2** of Scheme 1, was calculated to be strongly exothermic with a reaction enthalpy of −44.6 kcal/mol. The product from the insertion is the ethyl complex **2a** with a strong agostic interaction between nickel and a $\beta$-hydrogen. It appears that the insertion takes place with ethylene approaching **1a** in the chelate plane.

The second insertion of ethylene, **S3**, results in the butyl complex, **IV**, for which the most stable conformation was found to be **3c** with a strong agostic interaction between nickel and a $\beta$-hydrogen. The process **2a** + $C_2H_4$ → **3c** has a calculated reaction heat of −25 kcal/mol. Thus, the total formation of the butyl complex **3c** from **1c** and two ethylenes is exothermic by 69.6 kcal/mol.

The final step in the dimerization cycle is the reaction between the butyl complex **IV** and ethylene, **S4**, of Scheme 1. This reaction generates 1-butene and recovers the $\pi$-complex **II**. Our investigation suggests that it is the ethyl complex **2a** rather than $\pi$-complex **II** that is regenerated in the catalytic cycle. We propose that the elimination of 1-butene, and regeneration of **2a**, takes place according to eq 6b via the mechanism outlined in Scheme 2. The reaction in eq 6b is calculated to be nearly thermoneutral with a modest endothermicity of 0.1 kcal/mol. The corresponding activation energy for the elimination process was estimated to be 17 kcal/mol.

We have finally carried out substitutions of hydrogen by $CH_3$ or $CF_3$ groups on the propanedialate(1−) ligand. It was found that such substitutions only had a minor effect on the thermochemistry of the insertion processes in the dimerization cycle.

**Acknowledgment.** We thank the Natural Sciences and Engineering Research Council of Canada (NSERC) for financial support. This work was supported in part by the donors of the Petroleum Research Fund, administered by the American Chemical Society (ACS-PRF No. 27023-AC3).